Structural Eng./Earthquake Eng., JSCE, Vol. 15, No. 1, 1s—9s, 1998 January
(J. Struct. Mech. Earthquake Eng., JSCE, No. 584/ I —42)

WAVE FIELD GENERATED BY LATERALLY VIBRATING SOURCE ATTACHED TO THE SURFACE OF ELASTIC HALF SPACE

Dong-Ho HA[1] and Hiromichi HIGASHIHARA[2]

[1]Member of JSCE, Ph.D., Research Engineer, Bridge Engineering Division, Kawasaki Heavy Industries, Ltd.
(Minamisuna 2-6-5, Koto-ku, Tokyo 136, Japan; formerly graduate student of the University of Tokyo)
[2]Fellow member of JSCE, Dr. of Eng., Professor, Earthquake Research Institute, The University of Tokyo
(Yayoi 1-1-1, Bunkyo-ku, Tokyo 113, Japan)

We analyzed the response of elastic half space to a harmonically vibrating lateral force applied to the surface. We first derived analytic formulae which give the wave field at an arbitrary depth. These formulae provide a theoretical basis for a new method of physical prospecting which has been developed recently and is believed to be crucial for the precision investigation of underground geological structure. Next we calculated the formula for the most important lateral mode. While a large response was generated at the surface in the form of surface waves, the radiation pattern showed remarkable directivity resulting a cone shaped strongly excited area with vertical axis beneath the source.

Key Words: *compliance of elastic half space, harmonically vibrating lateral force, artificial seismic source, directivity*

1. INTRODUCTION

The demand for precision investigation of underground geological structures is increasing because of the construction of huge civil structures, exploitation of resources, prediction of earthquakes and so on. There are many conventional methods. Boring which makes specimens and bore-holes is commonly performed for the site investigation. Sonar and the underground radar system are frequently used for engineering purposes with a limitation of sensing depth. Natural earthquakes, blast earthquakes, vibroseisms and air-guns are generally used by scientists. Natural earthquakes are a good source of geological information, but they are destructive and uncontrollable; i.e., its resolution is quite limited. The others also have many limitations in terms of the signal/noise (S/N) ratio, resolution and so on.

Recently, geophysicists have been discussing the possibility of a new method of active elastic-wave remote sensing of the upper crust of the earth[1)]. Artificial seismic sources will emanate continuous harmonic wave of small amplitude. Although signal is considered small, latest high performance seismographs with feedback control mechanism is expected not to miss the signal so long as the sources have practically reasonable ability provided by modern but conventional technologies.

This signal itself appears too small to be separable from the noise. But if the frequency of the emitted wave is kept constant for a very long period as several ten days or several months, we can cancel out the noises by stacking the data. The recent development of the GPS system and electro-mechanical control technologies has made such idea realistic, and models are now under field examination. These sources carry an electric motor and rotate an eccentric mass. Being adjusted continually by the time signal from GPS satellites, they have achieved constant frequency with error of less than 10^{-5}.

Another basic idea is the array-deployment strategy of the sources; individual source is regarded as an element of an enormous virtual source aperture. These sources are driven with a common identical frequency while the phase of each source is assigned in an appropriate manner which optimizes the prospecting mission. This

method enables a variety of different patterns of wave radiation.

This new concept requires a mathematical theory of compliance of elastic space ; it is necessary for the estimation of the needed power of the sources, the determination of the array geometry and the phase assignment among the sources. Takei and Kumazawa investigated the response of the elastic *full* space to various modes of oscillation[2] and they manufactured sources based on this knowledge.

They fixed the sources on the surface of the ground. Although the deployment of the sources deep in the ground is desirable, they will have to stay for the time being on the surface; the analysis of the response of the elastic half space is needed. The source attached to the surface of the ground will ordinarily generate surface waves. It may induce some secondary modes of oscillation. All these phenomena make worse the efficiency of the source and make the emitted wave dirty[3]. Analyses without accounting the interference at the surface of the ground are, therefore, insufficient for the new methodology. This is the objective of the present paper.

In this paper, analytical formulae are derived for all possible modes of oscillation. Next, the wave field induced by three kinds of sources is calculated: lateral source in full space, lateral source and torsional source attached to the surface of elastic half space. By using these results, we can design the sources and plan the optimal phased array system of the sources.

2. HISTORY OF THE MATHEMATICAL BASIS

The study of point load in elastic solids has a long history. One of the fundamental results in the theory of elasticity is the Kelvin's solution[4] for a force applied at a point in a solid of indefinite extent. The classical problem of Boussinesq[5] dealing with a normal force applied at the plane boundary of a semi-infinite solid is solved by superimposing solutions derived from Kelvin's results and Cerruti[6] investigated a tangential force case. The Mindlin solution[7] fills in the gap between the two by giving the displacement and stresses for a case where the force is applied near the surface. The solution is obtained similarly by superposition of a combination of nuclei of strain, which are derived by synthesis from Kelvin's solution.

The generation of elastic waves by the application of concentrated loads on the surface or inside of a half space is known as Lamb's problem[8] since Lamb was first to treat it. Most fully discussed were the surface motions generated by a line load and a point load applied normally to the surface. Both loads of harmonic time dependence and impulse were considered. Also truly ingenious and skillful introduction of a particular solution to loads inside the half space was shown. All the followers[9),10)] employed this method. Sezawa[9] extended Lamb's problem to arbitrary asymmetric modes with azimuthal dependency and suggested the general solution.

Since the study of Reissner[11], the surface source problem was mainly discussed as the response of a harmonically oscillating circular disk attached to the surface of an elastic body. A great many papers have been published while no special attention was paid to the behavior of the internal ground. One of the present authors developed a general inversion procedure of the Sezawa's formula in applying it to the circular disk on elastic half space[12]. It is applicable to the calculation of the response of the internal point.

The response of a homogeneous isotropic elastic full space to the harmonic lateral force is calculated by the following equation[13] that is originally from Kelvin's solution. The force acts in the x direction and u_x is the displacement response to the force direction.

$$u_x = \frac{1}{4\pi\rho} F_0 \left[-e^{\frac{i\omega R}{v_p}} \left\{ \left(\frac{3x^2}{R^3} - \frac{1}{R} \right) \left(\frac{1}{i\omega R v_p} + \frac{1}{\omega^2 R^2} \right) + \frac{x^2}{R^3 v_s^2} \right\} \right. \quad (1)$$
$$\left. + e^{\frac{i\omega R}{v_s}} \left\{ \left(\frac{3x^2}{R^3} - \frac{1}{R} \right) \left(\frac{1}{i\omega R v_s} + \frac{1}{\omega^2 R^2} \right) + \left(\frac{1}{R v_s^2} - \frac{x^2}{R^3 v_s^2} \right) \right\} \right]$$

where F_0 is the amplitude of the applied force, ρ is density, ω is circular frequency, R is distance, x is horizontal distance, v_s and v_p are S and P wave velocities respectively.

The response of the surface of elastic half space to a lateral excitation at the surface is expressed in the following equation[14],

$$u_x = \frac{F_0}{4\pi\mu} \int_0^\infty \left\{ \left(\frac{k}{\beta} - \frac{k\beta b^2}{F(k)} \right) J_0(kr) + \cos 2\theta \left(\frac{k}{\beta} + \frac{k\beta b^2}{F(k)} \right) J_2(kr) \right\} dk \quad (2)$$

where F_0 is the amplitude of the applied force, $F(k) = (k^2 + \beta^2)^2 - 4k^2\alpha\beta$, $\alpha = \sqrt{k^2 - a^2}$, $\beta = \sqrt{k^2 - b^2}$, $a = \omega/v_p$, $b = \omega/v_s$, r is horizontal distance, μ is rigidity and J_n is Bessel function of the first kind of order n.

Kobayashi reduced the infinite integral into a sum of a term expressing the contribution of the residue and an integral over a finite interval[15].

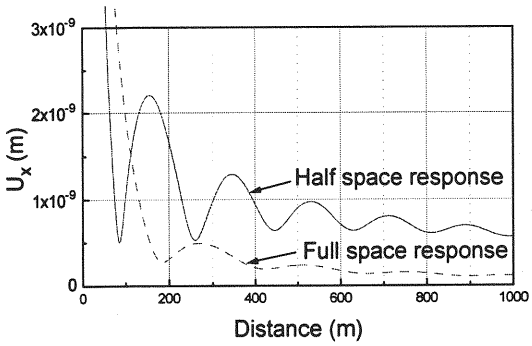

Fig.1 The comparison of responses of full space and half space with lateral force excitation

Fig. 1 is the comparison of responses of full space and half space with lateral force excitation, where $F_0 = (2\pi f)^2$ N and f = 5 Hz. Practically more higher frequency will be used but low frequency is applied for the convenience of the response comparison. If excitation frequency is increased, the response will be more complicated wave form. Twice the amplitude of force is used for the full space calculation. The absolute value of displacement response is shown in **Fig. 1**.

The far field response of the half space is much bigger than that of the full space. This means that a lot of energy of the emitted wave is trapped at the free surface as a surface wave; body wave generation of the surface source may be poor. Analysis of the recorded data will be difficult because the body waves which come up with information of deep underground is masked by the large amplitude surface waves. This is one of the critical issues.

3. FORMULA FOR THE WAVE IN ELASTIC HALF SPACE INDUCED BY A SUPERFICIAL POINT SOURCE

In this chapter, analytical formulae are systematically derived for the wave field generated in the elastic half space by a point source applied on the surface.

These formulae are based upon the general solution given by Sezawa[9], who obtained the following convenient and universal expression in cylindrical coordinates (r, θ, z),

$$u_r = \int_0^\infty \left\{ \begin{array}{l} -\dfrac{\partial J_m(kr)}{\partial r} A(k) e^{-\alpha z} \\ +\left[\dfrac{1}{r} J_m(kr) B(k) + \dfrac{\partial J_m(kr)}{\partial r} \beta C(k) \right] e^{-\beta z} \end{array} \right\} dk$$

$$u_\theta = \int_0^\infty \left\{ \begin{array}{l} \dfrac{1}{r} J_m(kr) A(k) e^{-\alpha z} \\ -\left[\dfrac{\partial J_m(kr)}{\partial r} B(k) + \dfrac{\beta}{r} J_m(kr) C(k) \right] e^{-\beta z} \end{array} \right\} dk$$

$$w = \int_0^\infty J_m(kr) \left[\alpha A(k) e^{-\alpha z} - k^2 C(k) e^{-\beta z} \right] dk \qquad (3)$$

where z = depth and other symbols are the same as in Eq. (2). The components of displacement in radial, circumferential and vertical direction are $u_r\cos(m\theta)$, $u_\theta\sin(m\theta)$ and $w\cos(m\theta)$ (m = 0, 1, 2, ···), respectively.

Similar integral representation of the stress components is obtained as a linear combination of first order derivatives of Eq. (3). Every possible solution is obtainable through integral transforms[13]. This comprehensiveness is valuable for the decomposition of the effect of interference with secondary modes from the recorded data.

(1) Case: $m = 0$

In this case, the torsional mode in which u_r and w vanish is separable from other modes. If a pure torque T around the z-axis is applied :

$$u_\theta = -\frac{T}{4\pi\mu} \int_0^\infty \frac{k}{\beta} e^{-\beta z} J_1(kr) dk \qquad (4)$$

This integral is analytically performable and results in the following expression:

$$u_\theta = -\frac{T}{4\pi\mu} \frac{r}{(r^2+z^2)} \left(\frac{1}{\sqrt{r^2+z^2}} + ib \right) e^{-ib\sqrt{r^2+z^2}} \qquad (5)$$

This is identical to the result of the pioneer work of E. Reissner [16].

There are two axisymmetric modes in which u_θ vanishes. The one is so-called vertical mode in which pure vertical force Q is applied.

$$w = -\frac{Q}{2\pi\mu} \int_0^\infty \left[k\alpha \frac{k^2+\beta^2}{F(k)} e^{-\alpha z} - 2\frac{k^3\alpha}{F(k)} e^{-\beta z} \right] J_0(kr) dk \qquad (6)$$

Although the vertical component of the displacement is prevailing, some horizontal (radial) displacement arises:

$$u_r = -\frac{Q}{2\pi\mu} \int_0^\infty \left[k^2 \frac{k^2+\beta^2}{F(k)} e^{-\alpha z} - 2\frac{k^2\alpha\beta}{F(k)} e^{-\beta z} \right] J_1(kr) dk \qquad (7)$$

The above two modes are physically realizable by means of a single source. According to the formula

obtained, there is another axisymmetric mode. This mode cannot be generated by a single source, but axisymmetric array of radially oscillating lateral sources can generate it.

(2) Case: $m = 1$

In this case, there is no separable component; three components always couple. The formulae become simpler in rectangular coordinates and let u_x and u_y be the displacement component in this coordinate system, and the formulae of all the modes takes the following form:

$$u_x = \frac{F_0}{4\pi\mu}(A + B\cos 2\theta) \qquad (8)$$
$$u_y = \frac{F_0}{4\pi\mu} B\sin 2\theta$$
$$w = \frac{F_0}{4\pi\mu} C\cos\theta$$

If a pure lateral force P is applied in x-direction, $F_0 = P$ and:

$$A = \int_0^\infty \left[-\frac{2k^3\beta}{F(k)} e^{-\alpha z} + \left(\frac{k}{\beta} + k\beta\frac{k^2+\beta^2}{F(k)}\right) e^{-\beta z} \right] J_0(kr)\,dk$$
$$B = \int_0^\infty \left[\frac{2k^3\beta}{F(k)} e^{-\alpha z} + \left(\frac{k}{\beta} - k\beta\frac{k^2+\beta^2}{F(k)}\right) e^{-\beta z} \right] J_2(kr)\,dk \qquad (9)$$
$$C = \int_0^\infty \left[\frac{2k^2\alpha\beta}{F(k)} e^{-\alpha z} - k^2\frac{k^2+\beta^2}{F(k)} e^{-\beta z} \right] J_1(kr)\,dk$$

If a pure moment M is applied around y-axis, $F_0 = 2M$ and:

$$A = \int_0^\infty \left[-k^2\frac{k^2+\beta^2}{F(k)} e^{-\alpha z} + \frac{2k\alpha\beta}{F(k)} e^{-\beta z} \right] J_0(kr)\,dk$$
$$B = \int_0^\infty \left[k^2\frac{k^2+\beta^2}{F(k)} e^{-\alpha z} - \frac{2k\alpha\beta}{F(k)} e^{-\beta z} \right] J_2(kr)\,dk \qquad (10)$$
$$C = \int_0^\infty \left[k\alpha\frac{k^2+\beta^2}{F(k)} e^{-\alpha z} - \frac{2k^3\alpha}{F(k)} e^{-\beta z} \right] J_1(kr)\,dk$$

This is the so-called rocking mode. As is in the axisymmetric case, there is another, third mode which cannot be produced by a single source but by an appropriate array of lateral mode sources.

4. WAVE FIELD GENERATED BY THE LATERAL MODE SOURCE

In this chapter, we calculate Eq. (9) of the most important lateral mode. This formula is an extension of Eq. (2).

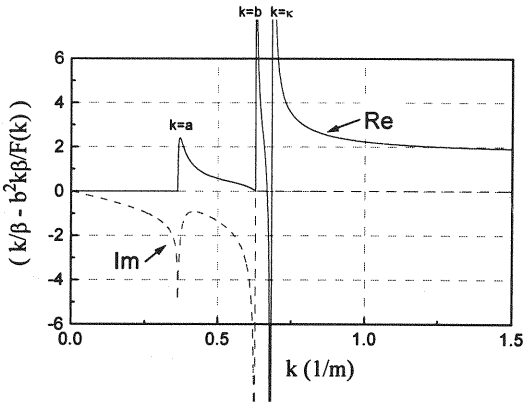

Fig.2 The integrand of a part of A in Eq. (11) without exponential and Bessel function

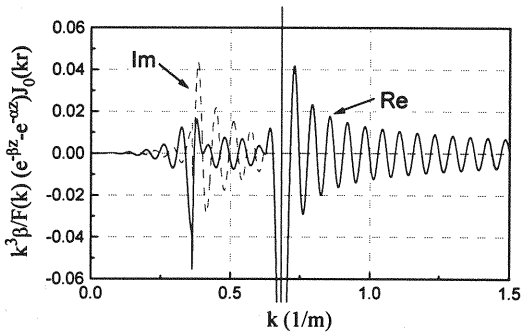

Fig.3 The integrand of a part of A in Eq. (11)

For the efficiency of the numerical calculation the terms of Eq. (9) are rearranged as Eq. (11).

$$A = \int_0^\infty \left[\left(\frac{k}{\beta} - b^2\frac{k\beta}{F(k)}\right) e^{-\beta z} + 2\frac{k^3\beta}{F(k)}\left(e^{-\beta z} - e^{-\alpha z}\right) \right] J_0(kr)\,dk \qquad (11)$$

Fig. 2 and **3** shows the integrand of the rearranged two parts of A in Eq. (11), where f = 50 Hz, v_s = 500 m/s, Poisson's ratio = 0.25, r = 100 m, z = 1 m. The infinite integral of the first part of Eq. (11) converges quickly because of the influence of exponential function. The second part of Eq. (11) shows bad convergence only when z is particularly small, but in such a case the proportion of this term in the total equation is small enough to be ignored. There are peaks at $k = a$ in the real and imaginary parts. Two singularities are found in the integral path: one is the root of the Rayleigh function $F(k)$, the other is $k = b$. Analytic and semi-analytic integration was done at these singularities with a

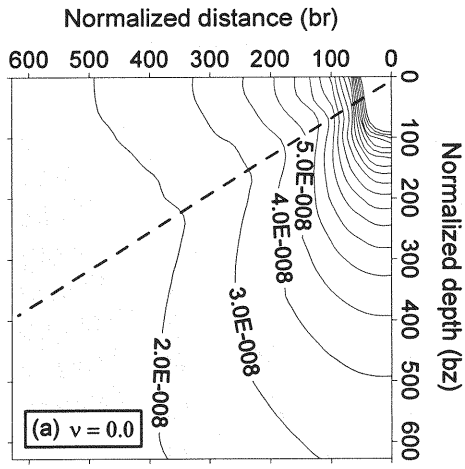

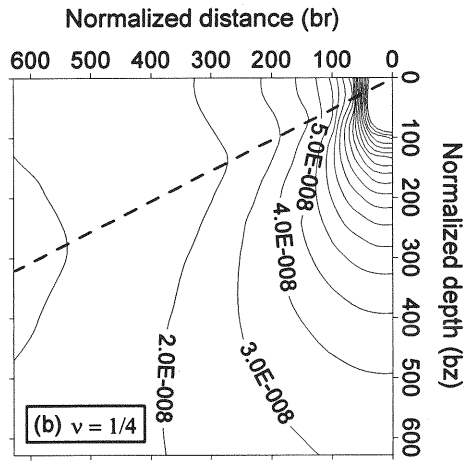

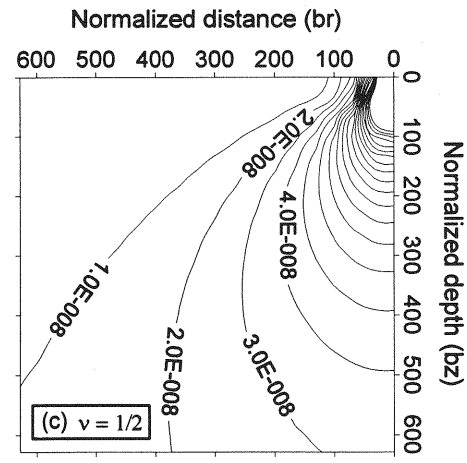

Fig.4 The response contour on full space

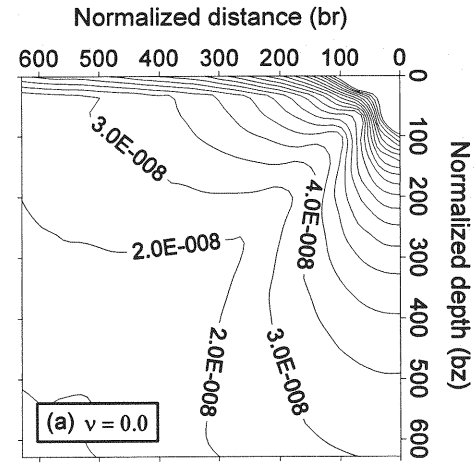

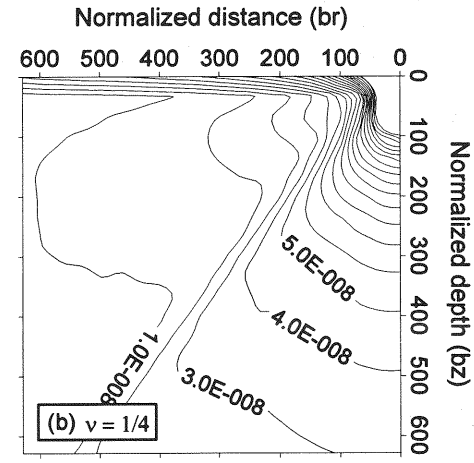

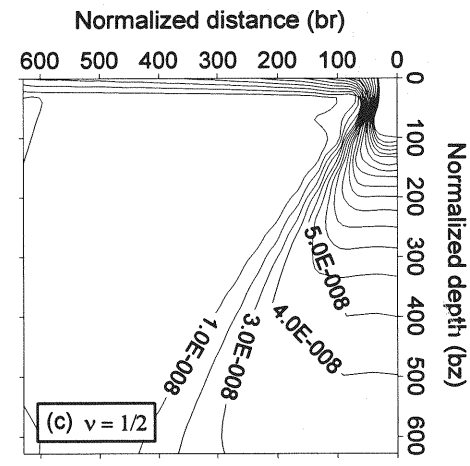

Fig.5 The response contour on half space

very short integral path. When $z = 0$, the contour integral procedure is possible as is shown in Kobayashi's paper[15]. When $z \neq 0$, such a procedure is impossible but no special integral skill is needed because $e^{-\beta z}$ makes the infinite integral converge quickly. The integral path was divided in many sub-paths in accordance with the peaks, singularities and the oscillating integrand. The error examinations of the integration were done in many ways.

By numerical integration we can obtain a complex-valued response which contains information about amplitude and phase.

The displacement responses of the force direction of the full space and of the half space induced by laterally vibrating sources are given as contour map in **Fig. 4** and **5**, where 50 Hz excitation, 500 m/sec S wave velocity, and normalized distance is used with three different Poisson's ratios. The three contours in **Fig. 4** are the responses of elastic full space and those in **Fig. 5** are the responses of elastic half space. Considering symmetry, 1/4 of the total contour map is shown in each contour of **Fig. 4** and 1/2 of the total contour map is shown in each contour of **Fig. 5**. The absolute value of the responses are shown in all contours. It is difficult to show the far-field and near-field responses together because of large difference of the value. The discussions here concern with far field responses only. For avoiding black part in contour map, we did not show the near field responses which have dense contour lines.

With the above parameters, normalized distance $br = 628$ and $bz = 628$ denote 1 km horizontal distance and 1 km vertical distance respectively. The response fluctuates with distance as shown in **Fig. 1** which is 5 Hz excitation case. Since 10 times larger excitation frequency is applied for contour drawing in **Fig. 4** and **Fig. 5**, the response fluctuates more quickly. For convenience of understanding the general attenuation tendency, smoothing (averaging) is done for contour drawing. The real part of the response of **Fig. 5(b)** is shown in **Fig. 6** in which distance and depth are 100 m, while distance and depth are 1 km in **Fig. 5(b)**. We can check the S wave length 10 m in depth direction.

Firstly, we consider the response contours of full space. Even though the compressibility is different, there is no response difference in the z direction as shown in the three contours in **Fig. 4**. The response in the force direction changes with the Poisson's ratio which becomes smaller as the Poisson's ratio becomes bigger. There are inversely curved parts in each of the contour lines that are convex to the direction of source. P wave and S wave have their own radiation patterns. These waves attenuate as r^{-1}.

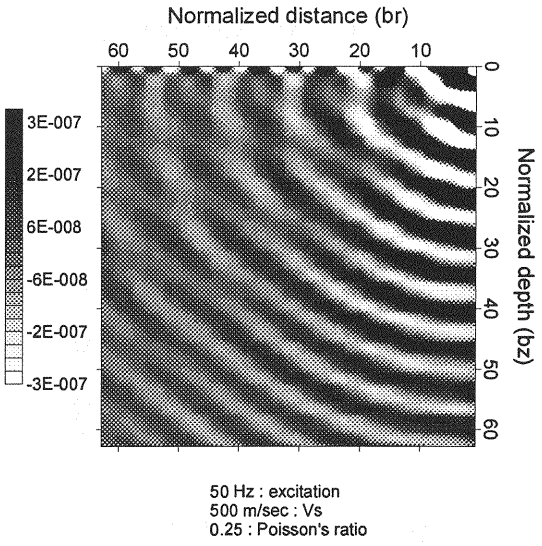

Fig.6 Real part of response with large scale

The magnitude of the P wave varies as the cosine of the angle between the force direction and the direction of the P wave. The magnitude of the S wave varies as the sine of the angle between the force direction and the direction of the S wave[17].

Thinking about the above radiation patterns, we can understand the response contour of full space. The response in the z direction comes from the magnitude of the S wave and the generation of this shear wave is not directly influenced by the Poisson's ratio as shown in **Fig. 4**. The response in the r direction comes from the magnitude of the P wave, and the generation of this compressional wave is largely influenced by the Poisson's ratio as shown in **Fig. 4**.

By looking into the contours in **Fig. 4(a)** and **(b)**, we can find the inversely curved parts, shown by dotted lines, in each of the contour lines which make diagonal parts with relatively small amplitude of response. Such a contour shape is from the radiation pattern of body waves which is written in preceding parts. The response of the upper part of this diagonal is mainly from the magnitude of the P wave, while the response of the lower part is mainly from the magnitude of the S wave. When the full space is incompressible, this diagonal becomes horizontal, as shown in **Fig. 4(c)**.

Secondly, we consider the response contours of half space. Large response is generated at the free surface of the half space. The responses in the z direction show the same value with different

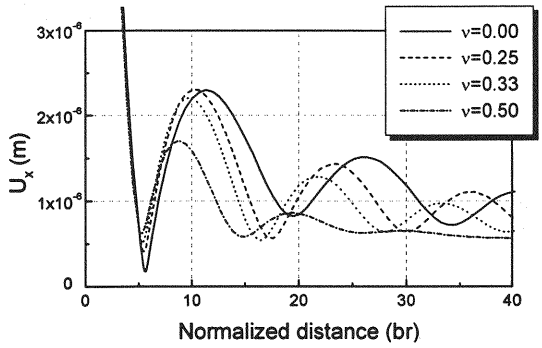

Fig.7 The surface responses with Poisson's ratio

Poisson's ratios as shown in the three contours of **Fig. 5**. We can find the diagonal lines in **Fig. 5(b), (c)** and the inversely curved parts in each of the contour lines in **Fig. 5(a)** as shown in the case of full space.

The large response on the surface in **Fig. 5** is considered to be the surface wave motion. The main part of this surface amplification is free surface Rayleigh waves, the depth of which is not clearly shown here for the convenience of contour drawing. The criterion for Rayleigh waves, i.e. exponential decay of displacement with the depth from the free surface, could be checked by using Eq. (8) and Eq. (9).

The absolute value of response of the free surface is shown in **Fig. 7** with four different Poisson's ratios. In the case of lateral source on half space, not only the amplitude of the surface response but also the phases of the surface response in the force direction are influenced by compressibility, as shown in **Fig. 7**. The surface response becomes smaller and smoother with the increase of the Poisson's ratio. The phase delay also changes slowly with a large Poisson's ratio.

We can find weak diagonal parts in **Fig. 5(a)** as shown in **Fig. 4(a), (b)**. The response of the lower part of this diagonal comes mainly from the magnitude of the S wave and the response of the upper part of this diagonal comes mainly from the magnitude of P wave, but the response of this part is smaller than that of full space. This phenomenon is due to the trapped energy on the free surface. Trapped means that a part of input energy is consumed by surface wave energy. This hinders us from emitting waves into deep underground.

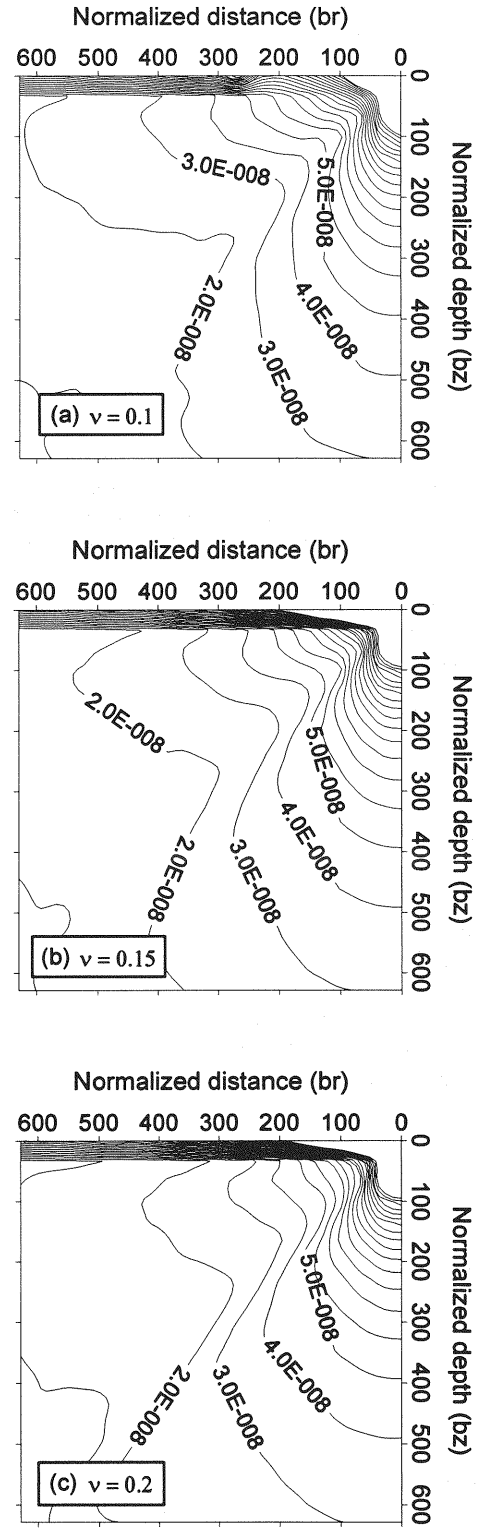

Fig.8 The response contour of half space with low Poisson's ratio

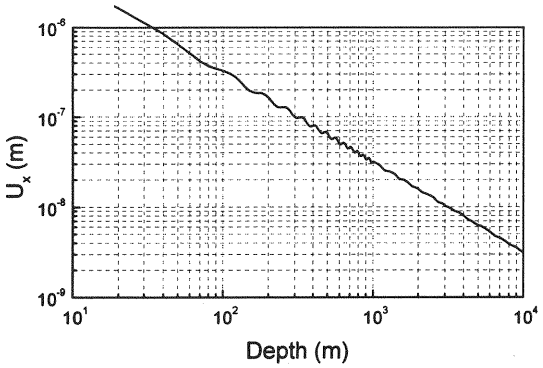

Fig.9 The response decay of half space with depth

The energy propagation of the upper part of the diagonal is mainly caused by P wave motion and much of the energy of that part is moved to the surface. On the other hand, the response of the lower part can be equal with that of full space. We examine this fact in the rest of this section. **Fig. 8** is the contours of the response of half space with a small Poisson's ratio which shows the absolute value of displacement response. The response on the upper part of the diagonal becomes smaller as the Poisson's ratio becomes bigger. Finally, the response of this part shows a large difference compared with that of the lower part. This large difference of response of the two parts causes the diagonal lines in **Fig. 5(b), (c)**.

The decay of the absolute value of response with depth is shown in **Fig. 9**. The absolute values of the responses in z direction in full space and half space are almost the same. Especially the absolute value of the response of full space in the far field can be approximated as follows,

$$\lim_{z\to\infty} \mid Eq.(1) \mid = \frac{1}{4\pi\mu}\frac{\mid F_0 \mid}{z} \qquad (12)$$

In the response of half space to surface source, the generation of S wave is almost same as in the full space case but the generation of P wave is poorer than in the full space case because the energy for P wave is trapped near the surface.

From the above results, we found the directivity of the response of elastic half space under the lateral source. This area of relatively large response has a cone shape whose axis is vertically downward from the source. In spite of the large trapped energy on the surface, the response of half space in this cone is almost the same as that of full space.

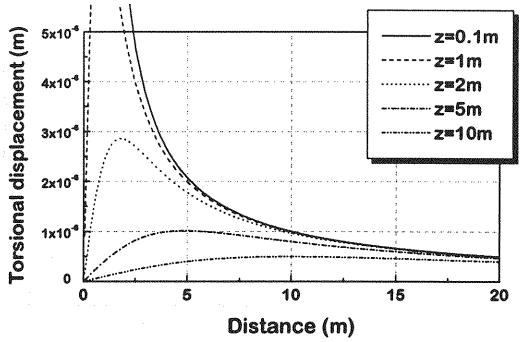

Fig.10 Torque response on half space

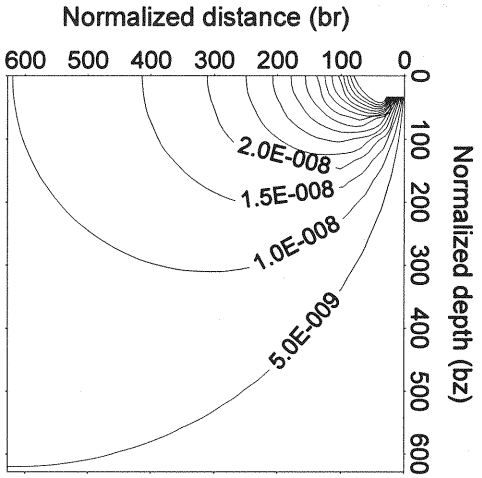

Fig.11 The response contour of torque on half space

5. THE WAVE FIELD INDUCED BY A TORSIONAL POINT SOURCE

The response of surface torque is examined here on the basis of Eq. (5).

The absolute value of the response to a torsional surface source is shown in **Fig. 10**. There is no large response on the surface in the response of the far field. The torsional response in the far field does not highly depend on depth.

A torsional source does not make surface wave. The response in the far field attenuates slowly with depth, besides the response near the source attenuates quickly with depth. When $r = 0$, i.e. down from the source, the response is zero.

The contour of the response of half space under torsional excitation on the surface is shown in **Fig. 11**, in which the absolute value of the response is used. Response decay with depth in the far field is very smooth and no free surface amplification is

found. The response under the source reduces quickly. The response decay of the torsional source with depth and radial distance is proportional to z^{-2} and r^{-1} respectively. The response magnitude to the lateral source is influenced by the magnitude of force and the response to the torsional surface source in the far field is proportional to not only the force magnitude of the source but also the excitation frequency.

It is difficult to make a large torsional source but the array system of lateral force unit can work as a large torsional source. By arranging lateral force units on a large circle, we can obtain the same response, in far-field, as that induced by torque. The new formula can be used for making such an array system.

6. CONCLUSION

In this paper, we analyzed the response of a homogeneous, isotropic, elastic half space to a harmonically vibrating point source applied to its surface, and derived analytically rigorous formulae of the response of the space at an arbitrary depth. These formulae provide a useful information to the design of new artificial seismic sources which have been developed recently.

Numerical integration was achieved for the lateral mode with high precision; a complex-valued response which contained the information about amplitude and phase was obtained. The result was compared with the response of two analytically solvable modes: the lateral mode of the full space and the torsional mode of the half space.

The obtained results are summarized as follows:

(1) Large response is generated at the surface in the form of surface waves. This type of response does not exist in the case of the full space nor in the case of the torsional mode of the half space.

(2) The radiation pattern shows remarkable directivity. The large response area has a cone shape with a vertical axis beneath the source.

(3) Owing to this directivity, in spite of the large energy trapping at the surface, the response decay of the lateral mode with depth in the far field is almost the same as that of the full space case.

(4) A relatively large response area of the torsional mode is skewed to the side down with weak response beneath the source. The response decay of the torsional mode is reciprocally proportional to both the horizontal distance and the square of the depth.

(5) The response to the torsional surface source in the far field is proportional to the excitation frequency and force amplitude of the source. The response to the lateral surface source is influenced by the force amplitude alone.

ACKNOWLEDGMENT: We thank Prof. Mineo Kumazawa for his discussion. For this study, we have used the computer systems of Earthquake Information Center of Earthquake Research Institute, University of Tokyo.

REFERENCES

1) Kumazawa, M. and Takei, Y.: Active method of monitoring underground structures by means of ACROSS, *Programme and Abstracts, The Seismological Society of Japan*, No.2, 1994.

2) Takei, Y. and Kumazawa, M.: Phenomenological representation and kinematics of general seismic source including the seismic vector modes, *Geophy. J. Int.*, No.121, pp.641-662, 1995.

3) Ha, D.H. and Higashihara, H.: The comparison of single force response on full and half space, *Programme and Abstracts, The Seismological Society of Japan*, No.2, 1995.

4) Kelvin, L.: Displacement due to a point load in an indefinitely extended solid,: *Mathematical and Physical papers*(London), Vol.1, 1848.

5) Boussinesq, J.: *Applications des potentiels a l'etude de l'equilibre et du mouvement des solides elastique*, Paris, Gauthier-Villars, 1885.

6) Cerruti, V.: *Ricerche intorno all' equilibrio dei corpi elastici isotropi*, Accademia Nazionale dei Lincei, Men. fis. Mat., Roma, 1882.

7) Mindlin, R.D.: Force at a point in the interior of a semi-infinite solid, *Physics*, Vol.7, pp.195-202, 1936.

8) Lamb, H.: On the propagation of tremors over the surface of an elastic solid, *Philosophical transaction of Royal Society of London, Ser.A*, Vol.203, pp.1-42, 1904.

9) Sezawa, K.: Further studies on Rayleigh-waves having some azimuthal distribution, *Bulletin of the Earthquake Research Institute*, Vol.6, pp.1-18, 1929.

10) Matsuoka, O. and Yahata, K.: Basic analysis on problems of a three dimensional homogeneous, isotropic, elastic medium, and the applications, part[3], *Transactions of Architectural Institute of Japan*, No.298, pp.43-53, 1980.

11) Reissner, E.: Stationare, axialsymmetrische, durch eine schuttelnde masse erregte schuingungen eines homogenen elastischen halbraumes, *Ingenieur-Archiv*, Vol.7, pp.381-396, 1936.

12) Higashihara, H.: Direct integral equation method of forced horizontal vibration of circular disk on elastic half space, *Proc. of JSCE*, No.374/I-6, pp.523-530, 1986.

13) Achenbach, J.D.: *Wave propagation in elastic solids*, North-Holland Publishing Company, 1973.

14) Tajimi, H.: Basic theories on aseismic design of structures, *Report of the Institute of Industrial Science, Univ. of Tokyo.* Vol.8, No.4, pp.170-215, 1959.

15) Kobayashi, T.: Evaluation of response to point load excitation on semi-infinite medium, *Transactions of Architectural Institute of Japan*, No.302, pp.29-35, 1981.

16) Reissner, E.: Freie und erzwungene Torsionsschwingungen des elastischen Halbraumes, *Ingenieur-Archiv*, Vol.8, pp.229-245, 1937.

17) Aki, K. and Richards, P.G.: *Quantitative seismology*, W.H. Freeman and Company, 1980.

(Received March 5, 1996)